

Isotopic Fingerprint of Electron-Phonon Coupling in High- T_c Cuprates

H. Iwasawa,^{1,2,*} J. F. Douglas,³ K. Sato,^{2,4} T. Masui,⁵ Y. Yoshida,² Z. Sun,³ H. Eisaki,² H. Bando,² A. Ino,⁶ M. Arita,⁷ K. Shimada,⁷ H. Namatame,⁷ M. Taniguchi,^{6,7} S. Tajima,⁵ S. Uchida,⁸ T. Saitoh,¹ D. S. Dessau,³ and Y. Aiura^{2,7,+}

¹Department of Applied Physics, Tokyo University of Science, Shinjuku-ku, Tokyo 162-8601, Japan

²National Institute of Advanced Industrial Science and Technology, Tsukuba, Ibaraki 305-8568, Japan

³Department of Physics, University of Colorado, Boulder, Colorado 80309-0390, USA

⁴Faculty of Science, Ibaraki University, Mito, Ibaraki 310-8512, Japan

⁵Department of Physics, Osaka University, 1-1 Machikaneyama, Toyonaka, Osaka 560-0043, Japan

⁶Graduate School of Science, Hiroshima University, Higashi-Hiroshima 739-8526, Japan

⁷Hiroshima Synchrotron Radiation Center, Hiroshima University, Higashi-Hiroshima 739-8526, Japan

⁸Department of Physics, University of Tokyo, Tokyo 113-8656, Japan

(Received 16 June 2008; published 9 October 2008)

Angle-resolved photoemission spectroscopy with low-energy tunable photons along the nodal direction of oxygen isotope substituted $\text{Bi}_2\text{Sr}_2\text{CaCu}_2\text{O}_{8+\delta}$ reveals a distinct oxygen isotope shift near the electron-boson coupling “kink” in the electronic dispersion. The magnitude (a few meV) and direction of the kink shift are as expected due to the measured isotopic shift of phonon frequency, and are also in agreement with theoretical expectations. This demonstrates the participation of the phonons as dominant players, as well as pinpointing the most relevant of the phonon branches.

DOI: 10.1103/PhysRevLett.101.157005

PACS numbers: 74.70.-b, 74.25.Jb, 79.60.-i

The effects of electron-boson interactions on electronic self-energies show up as sudden changes in the electron dispersion, or “kinks,” via angle-resolved photoemission spectroscopy (ARPES) [1,2]. While the kinks are now indisputable, their origin as arising from electronic coupling to phonons [3–5], magnetic excitations [6–9], or both [10], remains unclear. The best way to identify the origin of an interaction is to slightly modify the interaction in a controlled manner. For phonons, this can be done via an isotopic exchange, which varies particle masses and hence the vibrational energies. Here we substitute the oxygen isotopes ($^{16}\text{O} \rightarrow ^{18}\text{O}$) leading to a softening of phonon energies of a few meV [$= \Omega(1 - \sqrt{16/18})$] where Ω are the bare phonon frequencies of 40–70 meV [11,12]. Recent STM experiments showed an isotopic shift of a second derivative feature of 3.7 meV [13], though whether the observed shift is evidence for electron-phonon coupling has been disputed by a number of groups in terms of the inelastic tunneling barrier [14–16]. Even earlier than that, Gweon *et al.* used ARPES to study isotope effects on the electronic structure [17]. They found that the primary effect was at high energy and was unusually strong (up to 30 meV), though these results were not reproduced by more modern experiments [18,19]. For the effect on the kink scale they presented a roughly 5–10 meV isotopic softening but about 2–3 times larger than one of observed in STM. Therefore, a direct and clear “fingerprint” of strong electron-phonon interactions in the high- T_c superconductors has been missing up to now.

The momentum selectivity of ARPES brings an additional tool to bear on the study of the isotope effect which is not available from tunneling. This information is very helpful in separating out the energy and momenta of the

bosonic modes which couple most strongly to the electronic degrees of freedom. Here we focus on the “nodal” spectra, i.e., those along the $(0,0)$ - (π,π) direction in the Brillouin zone where both the superconducting gap and pseudogap are minimal or zero [1,2]. This is the portion of the Brillouin zone where the kinks or self-energy effects have been most strongly studied both experimentally [3,20,21] and theoretically [22,23]. As described very recently by Giustino *et al.* [24] and Heid *et al.* [25], there is still great controversy about the nature of the coupling in this direction; these two theoretical arguments imply that the phonon coupling could only be a minor player in the overall electron-boson coupling of these states because the calculations indicate a significantly weaker kink than what is found in experiment.

Analysis and interpretation of the nodal data are also more straightforward than the data throughout the Brillouin zone, as the energies of any bosonic modes in the spectra are expected to be shifted by the energies of the gaps. Assuming any isotope shifts go roughly as [$\Omega(1 - \sqrt{16/18})$], these are at most a few meV, requiring an unusually high-precision ARPES experiment. To verify such a tiny effect in the most convincing way, we utilized bulk-sensitive low photon energy ARPES (LEARPES), which has greatly improved spectral resolution compared to “conventional” ARPES [26]. In this Letter, we report an isotopic fingerprint of electron-phonon coupling as a clear isotope shift of the kink energy taking advantages of LEARPES. Present results provide straightforwardly that the origin of the nodal kink is due to the electron-phonon interactions.

High-quality optimally doped $\text{Bi}_2\text{Sr}_2\text{CaCu}_2\text{O}_{8+\delta}$ (Bi2212) single crystals were prepared by the traveling-

solvent floating-zone technique [27]. Oxygen isotope substitution was performed by annealing procedures (R-Dec Co. Ltd., ASF-11T) [28], yielding a slight decrease of T_c from 92.1 to 91.1 K. A softening of the oxygen vibration modes and the high oxygen isotope substitution rate (more than 80%) was confirmed by Raman spectroscopy [29]. Further, LEARPES gives us unparalleled precision in determining the Fermi surface areas directly from the Fermi surface maps, and we have confirmed that these are the optimal and the same for the two isotopes to the level below 2% (a doping level uncertainty $\Delta x = 0.003$).

The present data were collected at BL-9A of Hiroshima Synchrotron Radiation Center using a Scienta R4000 electron analyzer. We used our newly developed high-precision 6-axis sample manipulator to remove the extrinsic effect due to a sample misalignment. The clean and flat surface of the samples was obtained by cleaving *in situ* in ultrahigh vacuum better than 4×10^{-11} Torr below 10 K. The total instrumental energy and angular (momentum) resolutions were better than 5 meV and 0.4° (0.005 \AA^{-1}) at 7.0 eV photons, respectively.

First, we optimized the excitation energy to avoid the complications in extracting accurate band dispersions due to the very small but finite (0.01 \AA^{-1}) bilayer splitting, which is now known to exist even along the nodal line [Figs. 1(a) and 1(b)] [30]. By tuning the photon energy to 7.0 eV, we can see the complete isolated and individual antibonding band dispersion [Figs. 1(c) and 1(d)], giving the extremely fine quasiparticle dispersion with the momentum full width (Δk) below 0.005 \AA^{-1} [black (blue) line in Fig. 1(e)]. This is in sharp contrast to the cases of the dispersion with bilayer splitting [Fig. 1(b)], and also to the

conventional ARPES spectra broadened by a limit of resolutions as well as the unresolved bilayer splitting [Fig. 1(f)]. These advantages of LEARPES, including the band selectivity, are mandatory to verify the subtle change in the ARPES spectra with isotope substitution.

Figure 2(a) compares the ^{16}O (blue lines) and ^{18}O (red lines) energy-momentum dispersions derived from the momentum distribution curves (MDCs) near the nodal region taken with 7.0 eV photons. We found a very small isotope effect around the kink in the dispersions, independent of the cut position. We emphasize here that each of the five positive dispersions is exactly identical with each of the five negative dispersions for both ^{16}O and ^{18}O [as seen in Fig. 2(b)], which rules out the possibility of an extrinsic effect due to a sample misalignment. It should be noted that the present results are consistent with our previous ARPES [18,19], though we cannot see a convincing evidence of such a tiny isotope effect in there. This should be attributed to the fact that the experimental resolutions and/or accuracy were still not enough to observe a few meV order effect.

To visualize the subtle isotope effect more clearly, we deduced the real part of the self-energy $\text{Re}\Sigma(\omega)$. We extracted $\text{Re}\Sigma(\omega)$ by subtracting a bare band dispersion from the experimental one using three different forms of bare band in this analysis: linear [presented in Fig. 2(b)] [31], second order polynomial [32], and third order polynomial. It is worth noting that the present result is robust in regard to this choice. As seen in Fig. 2(b), clearly observed is a few meV isotopic shift of the ~ 70 meV peak of $\text{Re}\Sigma(\omega)$. Here we estimated the kink energy as the energy giving the peak maximum of $\text{Re}\Sigma(\omega)$, which was obtained

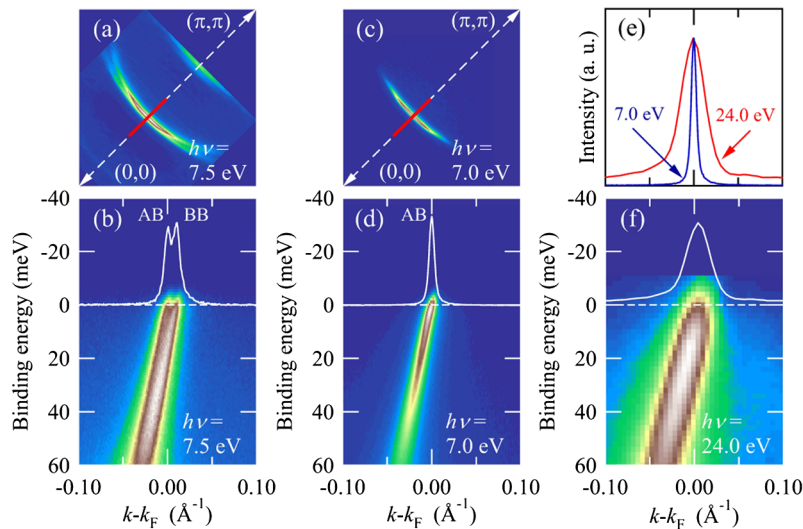


FIG. 1 (color online). (a),(c) Fermi surface maps taken with 7.5 and 7.0 eV photons, respectively. (b),(d),(f) Energy-momentum distribution maps taken with 7.5, 7.0, and 24.0 eV along the nodal direction, indicated by the gray (red) line in (a) and (c). MDCs at the Fermi level (E_F) are also shown by the white line, where the *BB* and *AB* denote bonding band and antibonding band, respectively. The Fermi momentum is set to the momentum of the *AB* crossing E_F . (e) Comparison of MDCs at E_F between 7.0 eV (blue line) and 24.0 eV (red line). Note that ARPES data using a conventional photon-energy of 24.0 eV were taken at BL5-4 of the Stanford Synchrotron Radiation Laboratory.

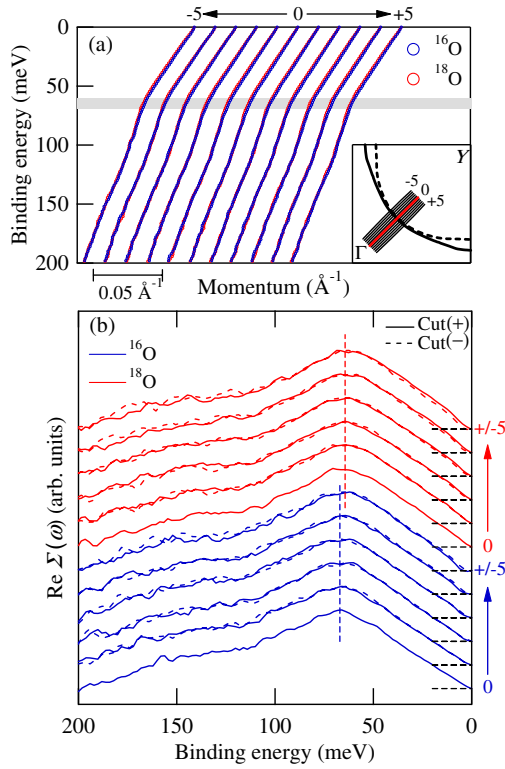


FIG. 2 (color online). (a) Energy-momentum dispersions near the nodal region both for ^{16}O (blue lines) and ^{18}O (red lines) from optimally doped Bi2212. Those measured cuts are labeled -5 to $+5$, displayed in the inset. Gray shaded area roughly indicates the kink in all the dispersions. (b) Real parts of the self-energy both for ^{16}O [blue (lower) lines] and ^{18}O [red (upper) lines], showing an isotope shift of ~ 70 meV peak. Blue dashed lines and red dashed lines indicates the kink energy, averaged from cut -5 to cut $+5$, for ^{16}O and ^{18}O , respectively. Positive and negative cuts are represented by solid lines and dashed lines, respectively.

by fitting the top portion of $\text{Re}\Sigma(\omega)$ with a Gaussian. To quantify the energy scale of the kink as well as the isotopic kink shift, we have studied multiple samples systematically.

Figure 3(a) shows the real part of the self-energy $\text{Re}\Sigma(\omega)$ both for ^{16}O (blue lines) and ^{18}O (red lines) multiple samples. From these $\text{Re}\Sigma(\omega)$, we obtained kink energy plotted as a function of five different samples each for both ^{16}O and ^{18}O in Fig. 3(c). Error bars for each sample were determined from a statistical analysis, and are smaller than the overall (sample-to-sample) spread which is more dominated by systematics. We found a clear isotopic softening of the kink energy from about 69.0 meV to about 65.6 meV, or a softening of 3.4 ± 0.5 meV [33]. Additionally, we used a completely independent analysis method using the widths of the ARPES peaks. This analysis has the advantage of not having any assumptions about a bare band, such that the isotope effect should appear more straightforward. Thus we see a 3.2 ± 0.6 meV shift in the imaginary part of the self-energy $\text{Im}\Sigma(\omega)$ [Figs. 3(b)

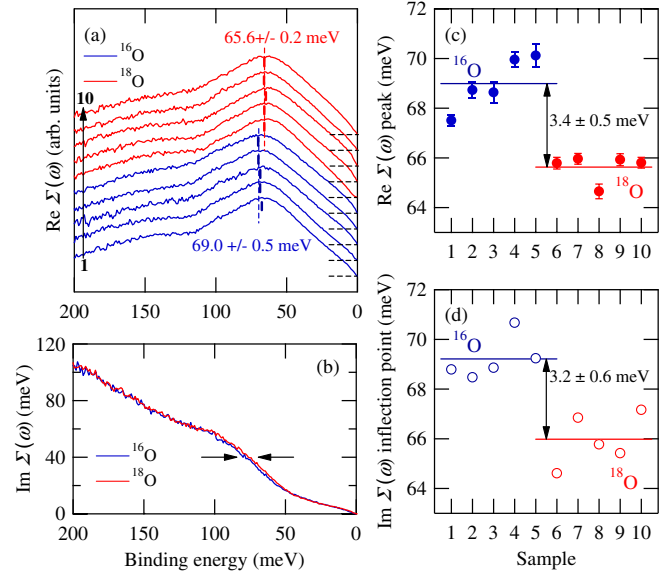


FIG. 3 (color online). (a) Real part of the self-energy $\text{Re}\Sigma(\omega)$ from five samples both for ^{16}O (blue lines) and ^{18}O (red lines) along the nodal direction indicated by the gray (red) line in Fig. 1(c). All $\text{Re}\Sigma(\omega)$ are deduced by subtracting a bare band dispersion from the experimental one, where ω is the energy relative to the Fermi energy, and normalized by the peak maximum, and are also offset for clarity. (b) Imaginary part of the self-energy $\text{Im}\Sigma(\omega)$ determined from MDC full widths. An impurity scattering term at $\omega = 0$ is subtracted as an energy independent constant background. (c),(d) Obtained kink energy as a function of sample numbers both for ^{16}O (blue line) and ^{18}O (red line) from $\text{Re}\Sigma(\omega)$ and $\text{Im}\Sigma(\omega)$, respectively.

and 3(d)]. By studying ten samples as well as by using multiple independent analysis methods, we compensated for possible systematic errors which might come into play when trying to determine energies to such a great precision. Further, we have also found a similar 3 meV isotope shift in the real and imaginary parts of the self-energy derived from the energy distribution curves. Therefore, we can state with confidence that the ~ 70 meV feature in the nodal electron self-energy is due to the coupling of the electrons with phonons. That this is the dominant feature in the electron self-energy, as is seen from both the real [Fig. 3(a)] and imaginary [Fig. 3(b)] parts of the spectrum, is clear and significant.

Then, which phonons are responsible for this coupling? Neutron scattering experiments [34] as well as first-principles phonon calculations [35] indicate a few phonon modes that are likely to be most relevant for the coupling: the in-plane “half-breathing” phonon mode ($\Omega \sim 70$ meV) and the “buckling or stretching” modes ($\Omega \sim 36$ meV). The apical oxygen stretching mode ($\Omega \sim 50$ meV) could also be considered, though calculations indicate that the number of allowed final states for these phonons is negligible [24]. By coupling the nodal electrons with momentum, \mathbf{k} , to other parts of the Fermi surface (\mathbf{k}'), the electron self-energy can in principle pick up the energy of the

superconducting gap $\Delta(\mathbf{k}')$ weighted over the Brillouin zone (and hence gap size) by the electron-phonon matrix elements $|g(\mathbf{k}, \mathbf{k}')|$, though there is still theoretical disagreement about how to do this gap referencing in a d -wave superconductor [36]. On the one hand, it is suggested that the kink energy appears at the mode energy plus the maximum gap energy, or $\Omega + \Delta_{\max}$ [37]. This scenario would indicate that the nodal kink is caused by the 36 meV buckling phonon. Alternatively, it is suggested that the kink represents simply the mode energy, indicating that the half-breathing phonon is dominant and couples electrons strongly along the node [24,25,38]. It is here that the present isotope effect is uniquely capable to distinguish the two.

For the buckling mode with $\Omega \sim 36$ meV, the isotope shift would be expected to be 2.1 meV, more than two error bars outside of the results published here. On the other hand, the breathing mode with $\Omega \sim 69$ meV would have an isotope shift of 3.9 meV, within the error bar of the isotopic shift seen here. This serves as a strong indication that the breathing mode is responsible for the nodal kink in ARPES data, consistent with expectations from recent theory [24]. However, the moderately strong coupling that we observe (a coupling parameter $\lambda \sim 0.6$ [39]) is significantly stronger than that calculated by theory [24,25], indicating that these calculations are missing an important ingredient to the electron-phonon coupling in the cuprates. Nominally we expect such enhancements in the electron-phonon coupling to originate in the strong electron correlation effects [40]—a problem which is interesting in its own right, but which also may have particular relevance to the mechanism of superconductivity in the cuprates.

In summary, we reported the isotopic fingerprint of the nodal kink probed by high-precision LEARPES. The present isotope shift of the kink energy provides the first convincing and direct evidence that the electron-phonon interactions are responsible for the origin of the nodal kink.

This work was supported by KAKENHI (19340105), DOE Grant No. DE-FG02-03ER46066, and Grant-in-Aid for COE research (No. 13CE2002) of MEXT Japan. The synchrotron radiation experiments have been done under the approval of HSRC (Proposal No. 06-A-15). H. I. acknowledges financial support from JSPS.

*Present address: Hiroshima Synchrotron Radiation Center, Hiroshima University, Higashi-Hiroshima 739-8526, Japan.

[†]To whom all correspondence should be addressed.
y.aiura@aist.go.jp

- [1] A. Damascelli, Z. Hussain, and Z.-X. Shen, *Rev. Mod. Phys.* **75**, 473 (2003).
- [2] J. C. Campuzano, M. R. Norman, and M. Randeria, in *The Physics of Superconductors*, edited by K. H. Bennemann and J. B. Ketterson (Springer, Berlin, 2004).
- [3] A. Lanzara *et al.*, *Nature (London)* **412**, 510 (2001).
- [4] Z.-X. Shen *et al.*, *Philos. Mag. B* **82**, 1349 (2002).
- [5] T. Cuk *et al.*, *Phys. Rev. Lett.* **93**, 117003 (2004).
- [6] D. J. Scalapino, *Science* **284**, 1282 (1999).
- [7] J. P. Carbotte, E. Schachinger, and D. N. Basov, *Nature (London)* **401**, 354 (1999).
- [8] H. He *et al.*, *Science* **295**, 1045 (2002).
- [9] K. Terashima *et al.*, *Nature Phys.* **2**, 27 (2006).
- [10] A. D. Gromko *et al.*, *Phys. Rev. B* **68**, 174520 (2003).
- [11] D. Reznik *et al.*, *Phys. Rev. Lett.* **75**, 2396 (1995).
- [12] R. J. McQueeney *et al.*, *Phys. Rev. Lett.* **87**, 077001 (2001).
- [13] Jinho Lee *et al.*, *Nature (London)* **442**, 546 (2006).
- [14] S. Pilgram, T. M. Rice, and M. Sigrist, *Phys. Rev. Lett.* **97**, 117003 (2006).
- [15] D. J. Scalapino, *Nature Phys.* **2**, 593 (2006).
- [16] J. Hwang, T. Timusk, and J. P. Carbotte, *Nature (London)* **446**, E4 (2007).
- [17] G.-H. Gweon *et al.*, *Nature (London)* **430**, 187 (2004).
- [18] J. F. Douglas *et al.*, *Nature (London)* **446**, E5 (2007).
- [19] H. Iwasawa *et al.*, *Physica (Amsterdam)* **463–465C**, 52 (2007).
- [20] T. Valla *et al.*, *Science* **285**, 2110 (1999).
- [21] X. J. Zhou *et al.*, *Nature (London)* **423**, 398 (2003).
- [22] P. Zhang, S. G. Louie, and M. L. Cohen, *Phys. Rev. Lett.* **98**, 067005 (2007).
- [23] M. L. Kulić and O. V. Dolgov, *Phys. Rev. B* **76**, 132511 (2007).
- [24] F. Giustino, M. L. Cohen, and S. G. Louie, *Nature (London)* **452**, 975 (2008).
- [25] R. Heid *et al.*, *Phys. Rev. Lett.* **100**, 137001 (2008).
- [26] J. D. Koralek *et al.*, *Phys. Rev. Lett.* **96**, 017005 (2006).
- [27] H. Eisaki *et al.*, *Phys. Rev. B* **69**, 064512 (2004).
- [28] We performed annealing under the same thermal conditions in either $^{16}\text{O}_2$ or $^{18}\text{O}_2$ gas: 700 °C for 168 h at 1.0 bar, followed by 700 °C for 168 h at 0.2 bar.
- [29] The isotopic shifts were observed in the B_{1g} mode in the CuO_2 layer, and also in oxygen vibrational modes in the BiO layer and the SrO layer. These shifts give the estimation of isotope exchange rates.
- [30] T. Yamasaki *et al.*, *Phys. Rev. B* **75**, 140513(R) (2007).
- [31] P. D. Johnson *et al.*, *Phys. Rev. Lett.* **87**, 177007 (2001).
- [32] W. Meevasana *et al.*, *Phys. Rev. Lett.* **96**, 157003 (2006).
- [33] The isotope shift was found to be insensitive to the choice of the bare velocity; the isotope shift shown here of 3.4 ± 0.5 meV utilized a linear bare dispersion, while a 3.3 ± 0.5 meV shift was found in the case of a second order polynomial.
- [34] L. Pintschovius, D. Reznik, and K. Yamada, *Phys. Rev. B* **74**, 174514 (2006).
- [35] K.-P. Bohnen, R. Heid, and M. Krauss, *Europhys. Lett.* **64**, 104 (2003).
- [36] A. Balatsky (private communication).
- [37] W. S. Lee *et al.*, *Phys. Rev. B* **77**, 140504(R) (2008).
- [38] T. P. Devereaux *et al.*, *Phys. Rev. Lett.* **93**, 117004 (2004).
- [39] The ratio of the “bare” dispersion in the absence of the kink to the renormalized dispersion due to the kink is $v_{\text{bare}}/v_F = 1 + \lambda \sim 1.6$.
- [40] S. Koikegami and Y. Aiura, *Phys. Rev. B* **77**, 184519 (2008).